Research Square

Preprints are preliminary reports that have not undergone peer review.
They should not be considered conclusive, used to inform clinical practice,
or referenced by the media as validated information.

Bacterial Cellulose Nanocrystal Networks in Biodegradable Films: Effects of Matrix Chemistry on Barrier Properties and Disintegration

Fabiola Medeiros
Mateus Abe
Pedro Nishimoto
Marcos Lorevice
Michel Brienzo
Fauze Aouada
Marcia Aouada

marcia.aouada@unesp.br

UNESP Faculty of Engineering of Ilha Solteira: Universidade Estadual Paulista Julio de Mesquita Filho Faculdade de Engenharia https://orcid.org/0000-0002-2534-5553

Research Article

Keywords: Gelatin, Pectin, HPMC, Sustainability, Water vapor permeability, Disintegration behavior

Posted Date: November 25th, 2026

DOI: https://doi.org/10.21203/rs.3.rs-11564794/v1

License: This work is licensed under a Creative Commons Attribution 4.0 International License.
Read Full License

ARTICLE

Bacterial Cellulose Nanocrystal Networks in Biodegradable Films: Effects of Matrix Chemistry on Barrier Properties and Disintegration

Authors: Fabíola Medeiros da Costa[a,b], Mateus Manabu Abe[c], Pedro Henrique Kenzo Nishimoto[d], Marcos Vinicius Lorevice[d,e], Michel Brienzo[c] Fauze Ahmad Aouada[a], Márcia Regina de Moura[a,*]

Authors affiliation:

a Hybrid Composites and Nanocomposites Group *(*GCNH), Department of Physics and Chemistry, School of Engineering, São Paulo State University (UNESP), Ilha Solteira 15385-000, SP, Brazil;

b University of Rio Verde (UniRV), Rio Verde, GO, Brazil;

c Institute for Research in Bioenergy (IPBEN), Rio Claro, SP, Brazil).

d Brazilian Nanotechnology National Laboratory (LNNano), Brazilian Center for Research in Energy and Materials (CNPEM), Campinas, Brazil

e School of Technology, University of Campinas, Campinas, Brazil

*** Correspondence: marcia.aouada@unesp.br; Tel.: +55-18-3743-1961**

Abstract

Incorporating bacterial cellulose nanocrystals (BCNCs) into biopolymer matrices is a strategy for modifying the functional properties of biodegradable films intended for food packaging applications. In this study, biopolymeric nanocomposite films based on gelatin, pectin, and hydroxypropyl methylcellulose (HPMC) were prepared by incorporating BCNCs obtained through the acid hydrolysis of bacterial cellulose by-products from a wound-dressing biorefinery. BCNCs concentrations were selected to fall below, near, and above the respective theoretical percolation thresholds, corresponding to 5%, 10%, and 15% for gelatin; 4%, 9%, and 14% for pectin; and 3.5%, 8.5%, and 13.5% for HPMC. The films were characterized in terms of optical transmittance, water vapor permeability, wettability, water absorption, Fourier-transform infrared spectroscopy (FTIR), thermal stability, and disintegration in natural soil and under composting conditions. Incorporation of BCNCs reduced water vapor permeability in the pectin and HPMC matrices, whereas the reduction observed in the gelatin matrix was not statistically significant. The presence of nanocrystals also reduced the films' moisture content and moderately increased the water contact angle, although all surfaces remained hydrophilic. Even at relatively high BCNCs concentrations, the films maintained high transmittance in the visible region—with values between 97% and 100% at 600 nm—while the incorporation of nanocrystals reduced transmittance in specific ultraviolet spectral regions, particularly in the gelatin and pectin films. FTIR analyses indicated the coexistence of characteristic bands from both the matrices and the BCNCs. The films exhibited high thermal stability, and disintegration behavior was strongly dependent on the nature of the matrix and the BCNCs concentration. Gelatin films underwent complete disintegration in soil, whereas pectin films were more resistant; HPMC films showed intermediate behavior. Under composting conditions, disintegration was accelerated for several formulations. The results demonstrate that the formation and organization of the BCNCs network can simultaneously modify barrier properties, water interaction, and structural stability, while matrix chemistry plays a decisive role in the disintegration behavior of the biopolymeric nanocomposites.

Keywords: Gelatin; Pectin; HPMC; Sustainability; Water vapor permeability; Disintegration behavior.

Introduction

The growing generation of plastic waste and the persistence of conventional fossil-based materials have driven the search for renewable, biodegradable alternatives that align with circular economy principles [1, 2]. In this context, biopolymeric nanocomposites have attracted interest for packaging applications, as they can combine the biodegradability and availability of biopolymers with enhanced performance through the use of nanofillers [3].

Among the biopolymeric matrices with potential for film production, gelatin, pectin, and hydroxypropyl methylcellulose exhibit complementary characteristics relevant to food packaging applications. Gelatin is a high-molecular-weight polypeptide composed of amino acids—primarily glycine (27%) and hydroxyproline/proline (25%) [4]. Pectin is a water-soluble heteropolysaccharide found mainly in plant cell walls and the luminal regions of plants and fruits; it is rich in β-(1-4)-D-galacturonic acid linked to significant amounts of galactose, arabinose, and rhamnose, and possesses excellent gel-forming capacity [5]. Hydroxypropyl methylcellulose (HPMC) is prepared by substituting hydroxyl groups with hydroxypropyl and methyl ether groups on the anhydroglucose backbone [6]. Despite these favorable characteristics, films composed exclusively of these biopolymers exhibit limitations, primarily regarding barrier properties. Thus, the incorporation of cellulose nanocrystals serves as a strategy to modify the structural organization of the matrices and promote interactions between the nanofiller and the biopolymers, enabling the production of materials with properties tailored to the specific application.

Among the various cellulosic nanofillers, bacterial cellulose nanocrystals (BCNCs) stand out due to their high degree of structural organization and the presence of surface hydroxyl groups—characteristics that facilitate their interaction with polymer matrices. Cellulose is a polysaccharide composed of D-glucose units linked by β-(1–4) bonds [7]; it can exist in various forms—such as nanocrystals, nanofibers, microcrystalline cellulose, and bacterial nanocellulose—which can be functionalized thanks to the presence of hydroxyl groups [8]. BCNCs are typically obtained by acid hydrolysis of the amorphous regions of microfibrils, thereby preserving the crystalline domains and forming highly ordered, rod-like structures [7, 9]. Due to the high density of surface hydroxyl groups and inter-particle interactions, these nanocrystals can form percolated networks capable of reinforcing the polymer matrix and facilitating load transfer [3]. Depending on the source, these nanocrystals offer a wide range of aspect ratios (L/d). However, if the level of adhesion between the filler (bacterial cellulose nanocrystals) and the matrix is insufficient, a diffusion pathway may arise. The existence of such a pathway is also linked to the connectivity of the filler and, consequently, to its percolation threshold [10]. Thus, concentrations below, near, and above the percolation threshold can yield different internal architectures and, consequently, different functional responses. In this regard, the use of BCNCs obtained from by-products of a wound-dressing biorefinery also expands the potential for valorizing cellulosic waste and developing materials with higher added value [3].

This study complements the work previously published by da Costa et al. [3], in which biopolymeric nanocomposite films were prepared by incorporating BCNCs at concentrations below, near, and above their theoretical percolation thresholds—previously determined as 14,

12.4, and 12 wt.% for gelatin, pectin, and HPMC, respectively [3]. Specifically, gelatin films were formulated with 5, 10, and 15 wt.% of BCNCs (designated as $G_{5\%}$, $G_{10\%}$, and $G_{15\%}$, respectively); pectin films with 4, 9, and 14 wt.% ($P_{4\%}$, $P_{9\%}$, and $P_{14\%}$, respectively); and HPMC films with 3.5, 8.5, and 13.5 wt.% ($H_{3.5\%}$, $H_{8.5\%}$, and $H_{13.5\%}$, respectively). Control films were designated as G_0, P_0, and H_0. In all cases, the total biopolymer concentration in the film-forming solution was fixed at 2.0% w/w, and the dry mass of BCNCs was calculated relative to the dry weight of each biopolymer matrix.

Although the formation of a percolated network of BCNCs can contribute to film reinforcement [3], this does not necessarily result in a simultaneous improvement of all the properties required for food packaging. The organization of the nanocellulosic network, the interaction with the matrix, and the formation of tortuous paths can alter the diffusion of fluid molecules, while changes in the film's structure and density can affect its transparency, protection against ultraviolet radiation, and water vapor permeability. These properties are particularly relevant for food preservation, since exposure to moisture and radiation can promote chemical, microbiological, and sensory changes, compromising the quality and shelf life of the product [11–14]. Another important characteristic of cellulose nanocrystals (CNCs) is their adjustable surface chemistry, which allows for adapting the physicochemical properties to meet specific demands; For example, the presence of these nanocrystals can influence the biodegradation of biopolymeric nanocomposites not only through alterations in the structure and accessibility of the polymer matrix, but also through potential interactions with the microbial community. Studies demonstrate that CNCs can exhibit antimicrobial activity associated with physical contact stress and destabilization of the bacterial membrane. Thus, the incorporation of CNCs into a biodegradable matrix can—depending on the concentration, the surface characteristics of the nanoparticles, and the structure of the nanocomposite—modify microbial colonization and the activity of microorganisms responsible for degradation. Consequently, the presence of a percolated CNC network can contribute to reducing the matrix's accessibility to enzymes and potentially altering the material's biodegradation dynamics [15]. Given this, the present study aimed to prepare and characterize biopolymeric nanocomposite films based on gelatin, pectin, and HPMC reinforced with BCNCs—obtained via acid hydrolysis (H_2SO_4) from wound dressing biorefinery by-products—and to evaluate the effect of nanocellulose network formation on opacity, water vapor permeability, wettability, water absorption, FTIR spectra, thermal properties, and, mainly, biodegradability (given the lack of biodegradation assays in the literature), with the goal of developing biodegradable films with suitable barrier properties for food packaging applications.

Experimental

Materials

Gelatin (CAS 9000-70-8; Dinâmica Química Contemporânea, Brazil), HPMC Methocel® K4M (CAS 9004-65-3; donated by Danisco Brasil Ltda; average methoxyl/hydroxypropyl ratio: 2.26), pectin (CAS 9000-69-5; kindly donated by CP Kelco, Brazil; degree of methoxylation > 50%), 64% v/v sulfuric acid (CAS 7664-93-9; Êxodo Científica, Brazil), dialysis membrane, Servapor Dialysis

tubing MWCO 12000-14, was purchased from Serva (São Paulo, Brazil), and potassium bromide (CAS 7758-02-3; Sigma-Aldrich, USA) were used without further purification. Biomedical-grade bacterial cellulose waste, synthesized by Gram-negative *Komagataeibacter xylinus*, obtained from the cutting of wound dressing films, was provided by Nexfill® (Brazil). Deionized Milli-Q water (Millipore Corp., USA; resistivity of 18.2 MΩ) was used in all analyses. The compost formulation materials (worm humus, rabbit feed, sawdust, and seed oil) and the cellulose paper were purchased from a gardening store, and the soil was collected from gardens at the São Paulo State University (UNESP) in Rio Claro/SP (coordinates: 22°23'45.18"S 47°32'49.18"W).

Extraction of bacterial cellulose nanocrystals

Bacterial cellulose nanocrystals (BCNCs) were extracted by acid hydrolysis, as described by de Costa et al. [3], and schematically presented in Figure 1. Briefly, the aforementioned BC (bacterial cellulose) was mechanically ground in a blender. The resulting powder was then hydrolyzed in sulfuric acid (64% v/v) using a ratio of 17.5 mL of solution per gram of BC. The mixture was kept at 50 °C under strong and constant stirring for 50 min. The reaction was quenched by diluting the mixture ten times with ice-cold water. The suspension was centrifuged at 600 rpm for 10 min, and the supernatant was discarded. The precipitate was transferred to the dialysis membrane (MWCO 12000-14) against Milli-Q water until the pH reached approximately 6. Finally, the BCNCs content was determined by the amount of total solids obtained after drying in an oven at 70 °C for 24 h.

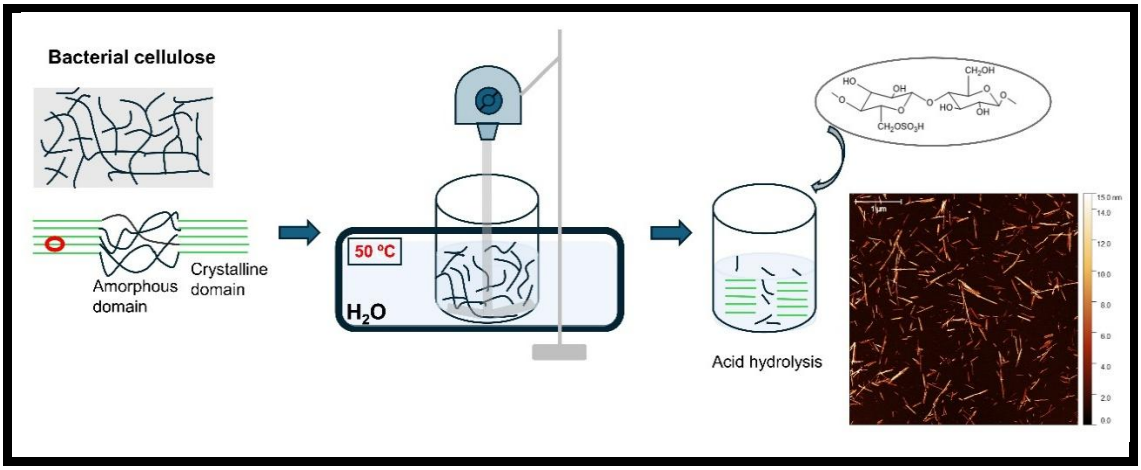

Figure 1: Simplified model of the extraction of nanocrystals from bacterial cellulose.

Optical property

The transparency of the films, at room temperature in 1 nm steps in the wavelength range of 200–800 nm, was determined using a UV 2600 spectrophotometer (Shimadzu, Japan) equipped with an integrating sphere attachment. The film sample (size 40 × 30 mm) was placed vertically in a cell; an empty cell was used as a reference.

Water vapor permeability

The water vapor permeability of the films was determined according to ASTM E96-95, with modifications [16].

A circular film sample (6 cm in diameter) was firmly fixed in a permeation cup containing 6 mL of distilled water. The relative humidity and ambient temperature of the test (inside the environmental chamber) were controlled at 50 ± 5% and 25 ± 5°C, respectively. The total test time was 25 hours. The sample was weighed at the beginning of the test and after 1, 2, 23, 24, and 25 hours. Five replicates were performed for each sample group.

Wettability

The film's wettability was measured through the water contact angle using a tensiometer, KSV Instruments (Helsinki, Finland). A drop of distilled water (6 µL) was deposited onto the sample (2.5 x 2.5 cm), and the contact angles were monitored for 60 s. The test was performed in quintuplicate. The average contact angle corresponds to the arithmetic mean of the angles determined at the right and left ends of the drop. The samples were left in a desiccator for 48 h before testing.

Water uptake

The water uptake content of the films was evaluated using the gravimetric method, in which the films were dried in an oven at 105°C for 24 hours (time required to reach constant weight). The percentage values of water uptake were determined as the fraction of weight lost during drying compared to the initial weight, and were reported on a wet basis. Equation 1 was used to calculate Pw (%) [9]:

$$Pw(\%) = \frac{Wi - Wf}{Wi} x100 \quad (1)$$

where P_w is the percentage of water uptake; W_i is the initial sample mass, and W_f is the final sample mass. The average measurements were taken.

Fourier transform infrared spectroscopy (FTIR)

FTIR spectra were recorded on a spectrophotometer (Nicolet NEXUS 670 FTIT), operating at 128 scans, frequency range of 400–4000 cm^{-1}, and 2 cm^{-1} resolution. Film samples were macerated with KBr and pressed into pellet form.

Thermogravimetry (TG)

The analyses were performed on an SDT Q600 instrument (TA Instruments) using approximately 5–6 mg of sample. The experiments were conducted with a heating ramp program from 20 to 600 °C, with a heating rate of 10 °C/min in a nitrogen atmosphere with a flow rate of 100 mL/min. All samples were placed in a desiccator for 48 h before testing to control moisture content.

Biodegradability

Disintegration on the soil surface

A laboratory-scale disintegration test was simulated to examine the biodegradability of the synthesized bioplastics. The test was conducted at the Biomass Characterization and Conversion Laboratory of the Bioenergy Research Institute (Ipben/Unesp), Rio Claro-SP.

The biodegradation/disintegration method consisted of placing the samples on the surface of a soil, and biodegradation was analyzed for 30 days by visual inspection alone, as measurements of biodegradation by mass loss have proven to be extremely difficult [17].

The soil was collected from the research institute's own gardens. Subsequently, the soil was sieved to remove synthetic and plant material.

The films were cut into 3.5 cm squares, dried and weighed, and then placed on top of 200 g of sifted soil in a polypropylene container approximately 64 mm long, 330 mm wide, and 85 mm deep. The containers were hermetically sealed.

The soil was maintained at 35% moisture and 30°C (DBO incubation). The tests were performed in duplicate. The controls in the test were: control film – film without contact with the soil and incubated at 30°C; soil control – soil without exposure to the film and incubated at 30°C.

Disintegration on the surface of the composting system

The film disintegration measurements on the surface of the composting system were based on the study conducted by Sánchez-Safont et al. [18], adjusted for laboratory scale by changing the temperature to 55°C and without adding starch to the composting formulation. This analysis was performed in duplicate with the films most resistant to disintegration in the soil.

The film dimensions were the same as in the previous test (disintegration in soil). The disintegration process was monitored through image recordings. The cellulose paper, as a positive control, was evaluated under the same conditions described previously for the film. The control films were exposed to the same temperature and composting time conditions, but not in contact with the compost, so that any disintegration and composting effect could be ruled out.

Statistical analysis

One-way analysis of variance (ANOVA) followed by Tukey's b-test was used to compare more than two datasets, after confirming the homogeneity of variances using Levene's test with Origin software, version 6.0 (Origin Lab, Northampton, MA, USA). All data are represented as mean ± standard deviation. Significant differences ($p \leq 0.05$) are denoted by showing the data provided in tables with different letters.

Results and discussion

Incorporation of biopolymers with BCNCs

Incorporating any substance into the film matrix can alter both the physicochemical characteristics of the packaging material and the quality attributes of the packaged food products, due to potential interactions between the components [3]. In polysaccharide-based polymers, these interactions largely depend on non-covalent cross-linking mechanisms, including hydrogen bonding, van der Waals forces, ionic interactions, and electrostatic interactions. However,

chemical cross-linking can also be achieved through the use of strong cross-linking agents, promoting structural modifications that enhance the functionality of these film-forming matrices [19]. In this context, incorporating cellulose nanocrystals into biopolymeric matrices represents a promising strategy, as the surface characteristics of the nanocrystals facilitate their interaction with various functional groups present in the polymer chains.

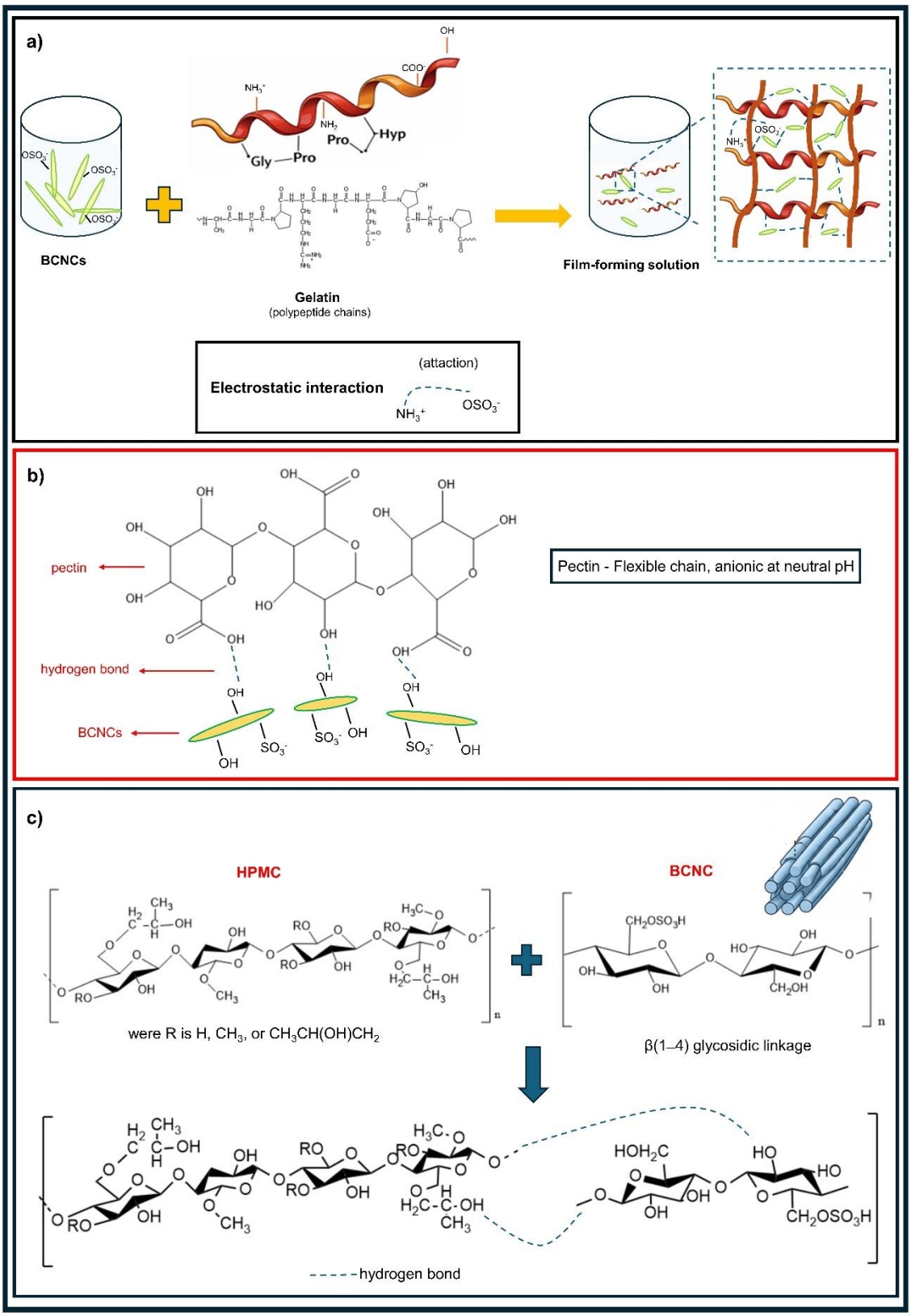

Figure 2: Illustration of BCNCs incorporated with gelatin (a), pectin (b), and HPMC (c).

Figure 2 presents a representative model of the incorporation of nanocrystals into biopolymeric matrices to form biopolymeric nanocomposite films. Cellulose nanocrystals exhibit inherent dispersibility in aqueous media and colloidal stability, without necessarily requiring

additives for electrostatic regulation. Furthermore, the abundance of functional groups exposed on their surface—particularly hydroxyl groups (–OH)—favors interactions with the polymer matrix chains, contributing to the organization of the nanocrystal–polymer interface and, consequently, to enhanced barrier properties and the introduction of additional functionalities [20]. Thus, although the surface characteristics of the cellulose condition the nanocrystal incorporation mechanism, the chemical nature of the matrix plays a fundamental role in defining the interactions established at the interface.

Among the structural parameters of nanocrystals that influence their ability to form a continuous network within the matrix, the aspect ratio (L/D) stands out, as it can be used to estimate the percolation threshold of BCNCs. For systems composed of elongated particles, a frequently used approximation relates the critical percolation volume fraction (V_{RC}) to the aspect ratio of the nanocrystals, as shown in Equation (2) [3, 21]:

$$V_{RC} = 0.7 \times \left(\frac{D}{L}\right) \quad (2)$$

where (V_{RC}) corresponds to the critical volume fraction required for the formation of a percolated network, (L) represents the average length of the BCNCs, and (D) corresponds to their average diameter. Based on the experimental value of (L/D = 6.67 ± 0.3), a critical volume fraction of approximately 10.49% (v/v) is obtained, corresponding to approximately 16.78% by mass [3]. This parameter is particularly relevant because, as the BCNCs concentration approaches the percolation threshold, the probability of contact between the nanocrystals increases, and consequently, so does the formation of an interconnected network within the matrix. However, the efficiency of this network depends not only on the concentration and aspect ratio of the BCNCs but also on the interactions established between their surface and the polymer's functional groups. BCNCs exhibit a negative surface charge due to the introduction of sulfate groups resulting from sulfuric acid hydrolysis, which enables electrostatic interactions with charged groups present in the matrix [22].

The interaction between BCNCs and gelatin can occur through molecular entanglement—promoting the formation of intermolecular hydrogen bonds—as well as through electrostatic interactions at the interface (Figure 2a). Gelatin chains possess protonated amino groups ($–NH_3^+$) and carboxylate groups ($–COO^-$), enabling electrostatic interactions between these charged species and the functional groups on the BCNCs surface. Concurrently, hydrogen bonding contributes to the formation of more stable interfacial complexes [23]. These interactions enhance compatibility between the gelatin matrix and the BCNCs, potentially improving the barrier properties of the films [24]. This effect is particularly significant near the calculated percolation threshold (16.78 wt% BCNCs / 14 wt% gelatin) [3]. Thus, the incorporation of BCNCs in a matrix of lower resistance, such as gelatin, can result in a structure that provides greater durability to the material [3, 25].

Similarly, the incorporation of BCNCs into pectin is facilitated by the high aspect ratio of the nanocrystals and the abundance of free hydroxyl groups on their surface, which can interact

with the functional groups of pectin chains—particularly carboxyl groups—via hydrogen bonding (Figure 2b). These interactions promote proximity between the two phases and can contribute to a more compact and homogeneous film structure [26]. This interaction was investigated at the molecular scale by Wu and Prasad [27], who demonstrated through molecular dynamics simulations that contact between CNCs and pectin promotes structural adaptation at the interface. According to the authors, while the internal regions of the CNCs preserve the crystalline organization characteristic of cellulose, the surface chains exhibit greater flexibility to accommodate pectin molecules. This rearrangement favors the formation of hydrogen bonds between cellulose hydroxyl groups and the hydroxyl and oxygen groups present in pectin, establishing a more cohesive interface between the two phases. Therefore, although the pectin–BCNCs interaction is predominantly non-covalent, the multiplicity of these interactions can facilitate stress transfer and the formation of a more compact nanocomposite network.

In turn, the incorporation of BCNCs into the HPMC matrix occurs at an interface characterized primarily by the presence of hydroxyl (–OH), methoxyl ($–OCH_3$), and hydroxypropoxyl groups on the polymer chains (Figure 2c). The polar groups of HPMC can form hydrogen bonds with the hydroxyl groups present on the BCNCs surface, promoting their dispersion and interaction with the matrix. Furthermore, the balance between the hydrophilic and hydrophobic moieties of HPMC can facilitate simultaneous interactions with different system components, contributing to the stability of the nanocrystal dispersion and reducing the tendency for aggregation or precipitation [28]. Thus, although all three systems utilize the same reinforcing agent—BCNCs—the distinct chemical characteristics of gelatin, pectin, and HPMC dictate different interfacial mechanisms; these mechanisms can influence nanocrystal dispersion, percolation network formation, and, consequently, the final properties of the biopolymeric nanocomposite films.

Optical property

The light transmittance of the films in the 200–800 nm range was measured to investigate their transparency and light-barrier properties. Figure 3 illustrates the behavior of ultraviolet and visible light beams incident on the biopolymeric nanocomposite samples.

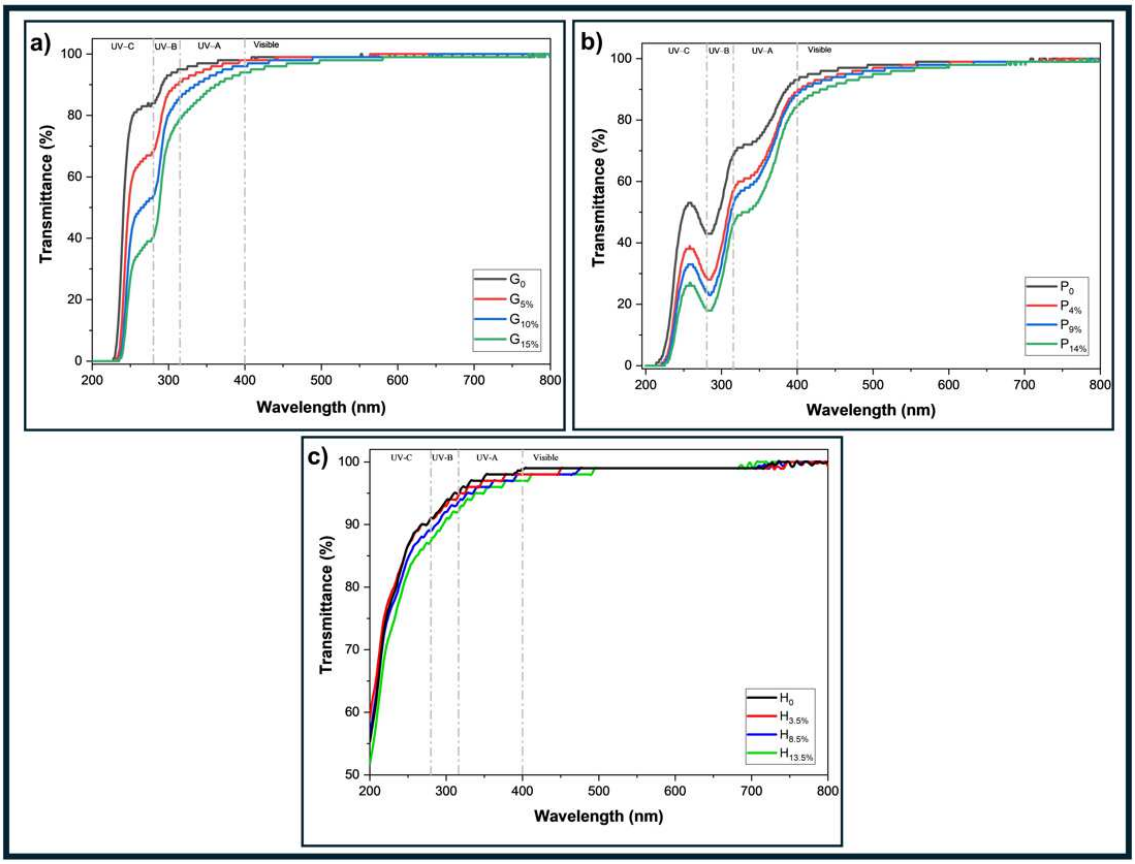

Figure 3: UV-vis transmittance spectra of biopolymeric nanocomposites based on gelatin (a), pectin (b), and HPMC (c).

UV radiation, in the range of 200–400 nm, is split into UV-A (315–400 nm), UV-B (280–315 nm), and UV-C (200–280 nm), as observed in Figure 3 [11, 13]. The pure films showed low protection against UV-A radiation due to the high transmittance values, and the addition of BCNCs increased protection against UV-A proportionally to the amount added, as shown in Figure 3. In the ranges of 280–315 nm (UV-B) and 200–280 nm (UV-C), the increase in the concentration of BCNCs in biopolymeric nanocomposites based on gelatin and pectin resulted in a reduction in light transmittance of the films. At 278 nm, the transmittance for the $G_{5\%}$ film was 68%, $G_{10\%}$ was 53%, and $G_{15\%}$ was 40% (Figure 3a). At 280 nm, the percentage of light transmitted by the pectin control film was 43%, with 29% for $P_{4\%}$, 24% for $P_{9\%}$, and 18% for $P_{14\%}$ (Figure 3b). In these ranges, such values suggest improved light barrier properties. This occurred because the structure of BCNCs can scatter light through the films [29]. Furthermore, Leite et al. [30] reported that the dispersion state of NCs affects the light transmittance of films, since the presence of micrometric agglomerates of NCs in films can scatter light, thus reducing light transmittance.

The analyzed pectin-based biopolymeric nanocomposites exhibited good UV barrier properties. A study by Ezati et al. [11] reported that pectin—a plant-derived polysaccharide—possesses suitable UV-protective properties, blocking approximately 70% of UV radiation due to the presence of carbonyl groups in its structure. Consequently, pectin has been used in conjunction with commercial synthetic polymers to impart UV-scattering properties.

Neat HPMC-based biopolymer films and nanocomposites (Figure 3c) offer little protection against UV-C light at wavelengths above 250 nm. UV-B, UV-A, and visible light continue to pass through them.

The transparency of the films is confirmed by the transmittance values between 97% and 100% at T_{600} (visible light transmittance) shown in Figure 3. Therefore, the difference in transmittance among the biopolymeric nanocomposite films at 600 nm can be considered negligible; both the pure films and the biopolymeric nanocomposites—even those with relatively high BCNCs loadings—exhibited low opacity, an observation also reported in the study by Li et al. [13] on fish gelatin films. Given that light transmittance exceeds 70% for all films, it can be inferred that these materials are suitable for practical applications and do not hinder consumer visibility of the food at the point of sale [12, 31]. Furthermore, it is widely recognized that film gloss and transparency noticeably impact the appearance of packaged food, making all the films suitable as direct packaging materials for food products; conversely, excessive light exposure can promote food oxidation and degradation [13].

Therefore, the formation of a percolated network of BCNCs can modify the optical properties of the films. At low concentrations, the nanocrystals are predominantly dispersed within the matrix, limiting the number of interfaces capable of promoting radiation scattering. As the BCNCs concentration increases, the formation of an interconnected structure at the percolation threshold can enhance the material's optical heterogeneity and promote light scattering [32].

Water vapor permeability (WVP)

The water vapor permeability of a film is a steady-state property that describes the rate of passage (transmission) of water vapor per unit area through the film subjected to a given relative humidity difference at a given temperature. Permeability depends on the diffusion (kinetic factor) and sorption (thermodynamic factor) of the penetrant, with water being the most common diffusing molecule. Water vapor transfer through hydrophilic films also depends on the partial pressure gradient; however, permeability is not an inherent property of hydrophilic films [33, 34].

The regulation of water vapor transfer between food and the external environment is one of the most important conditions affecting the quality of packaging materials [35]. Furthermore, a higher WPV value will increase water activity in food, leading to contamination and spoilage [12, 33]. When these films act as strong barriers against water vapor, this can significantly improve shelf life, quality, and food acceptance [29]. Therefore, it is necessary to keep the WPV as low as possible [34, 36–38].The WPV values of different gelatin, pectin, and HPMC films were evaluated, and the results are shown in Figure 4.

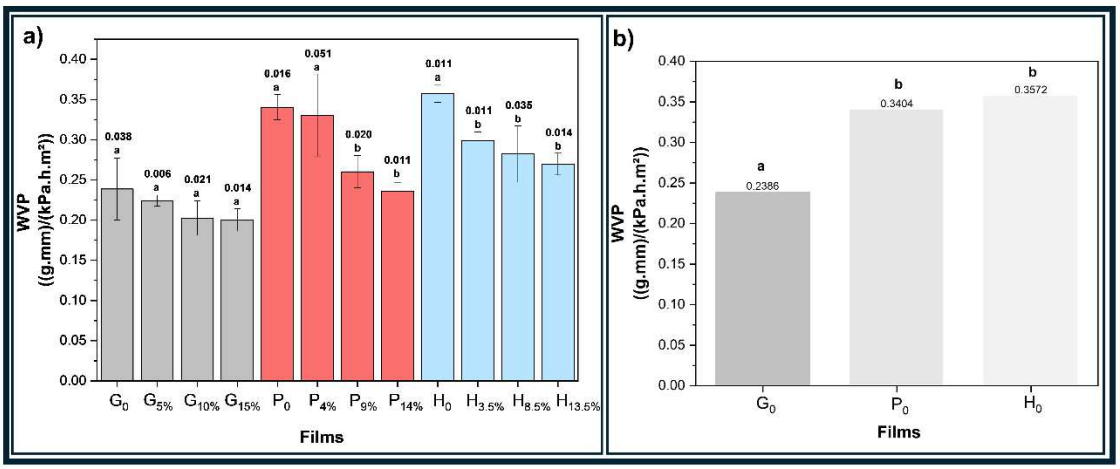

Figure 4: WVP of biopolymeric nanocomposites (a) and WVP of the matrices (b).

Compared to the unreinforced gelatin film (G_0), a trend of decreasing water vapor permeability (WVP) values was observed with the incorporation of BCNCs; however, this reduction was not statistically significant for any of the concentrations evaluated. The WVP of the control gelatin film was 0.2386 g.mm.kPa^{-1}.h^{-1}.m^{-2}, whereas the films containing BCNCs at concentrations of 5%, 10%, and 15% (w/w) exhibited values of 0.2242, 0.2026, and 0.2002 g.mm.kPa^{-1}.h^{-1}.m^{-2}, respectively (Figure 4a). The WVP values obtained in this study were lower than those reported by Oyeoka et al. [33], who evaluated gelatin and polyvinyl alcohol-based films reinforced with cellulose nanocrystals isolated from water hyacinth fibers.

The WVP of the control pectin film (P_0) was 0.3404 g.mm.kPa^{-1}.h^{-1}.m^{-2}. After the addition of 4%, 9%, and 14% (by mass) of nanocrystals, the permeability was 0.3306 g.mm.kPa^{-1}.h^{-1}.m^{-2}, 0.2602 g.mm.kPa^{-1}.h^{-1}.m^{-2}, and 0.2362 g.mm.kPa^{-1}.h^{-1}.m^{-2}, respectively (Figure 4a). These results indicate that the addition of BCNCs to pectin—at levels near and at the percolation threshold—had a positive effect on the WVP of the resulting biopolymeric nanocomposite films; this may be associated with the presence of crystalline domains. In P_0 films, water molecules permeate directly in a direction perpendicular to the film surface; however, in biopolymeric nanocomposite films, the nanocrystal network acts as a barrier, forcing water molecules to navigate around the BCNCs along a tortuous path. Consequently, the diffusion path length increases, and the diffusion rate decreases [35, 39].

The WPV values of the HPMC films can also be observed in Figure 4a. The addition of BCNCs significantly reduced (considering $p < 0.05$ relative to the control) the WPV of the films at the different concentrations studied. The results obtained were: H_0 0.3572 g.mm.kPa^{-1}.h^{-1}.m^{-2}, $H_{3.5\%}$ 0.2992 g.mm.kPa^{-1}.h^{-1}.m^{-2}, $H_{8.5\%}$ 0.2822 g.mm.kPa^{-1}.h^{-1}.m^{-2}, and $H_{13.5\%}$ 0.2698 g.mm.kPa^{-1}.h^{-1}.m^{-2}. These results can also be attributed to the presence of crystalline domains.

Analysis of variance (one-way ANOVA) indicated a significant difference ($p < 0.05$) in water vapor permeability (WVP) among the evaluated matrices, as shown in Figure 4b. The gelatin film (G_0) exhibited the lowest WVP value (0.2386 ± 0.0383 g.mm.kPa^{-1}.h^{-1}.m^{-2}), differing significantly from the pectin (P_0, 0.3404 ± 0.0156 g.mm.kPa^{-1}.h^{-1}.m^{-2}), and HPMC (H_0, 0.3572 ± 0.0107 g.mm.kPa^{-1}.h^{-1}.m^{-2}) films.

In the study by Wu et al. [40], it is noted that barrier properties are influenced by several factors, including the tortuosity of the path taken by gas molecules through the matrix, the dispersion of nanofillers, and the interactions between the nanofillers and the polymer matrix. Among these factors, nanofiller dispersion plays a predominant role, as inadequate distribution can compromise the material's efficiency in forming a barrier against gas transport. CNCs, in particular, are difficult to disperse stably in water due to strong intermolecular interactions, especially those involving hydrogen bonding. This poor dispersibility promotes nanoparticle aggregation and, consequently, limits improvements in the barrier properties of nanocomposite coatings. In this context, surface modification of CNCs serves as a strategy to enhance dispersion stability in aqueous media. The hydroxyl groups on the CNCs surface can serve as sites for chemical or physical modification, helping to reduce nanoparticle aggregation and promote a more homogeneous distribution within the matrix, which can enhance the barrier properties of biopolymeric nanocomposites [40].

Wettability

The wettability and hydrophilic/hydrophobic characteristics of the film surface were investigated by measuring the angle of contact with water. Figures 5a, b, and c show the average contact angle results for the left and right ends of the drop for different samples at t = 0 s (initial time).

In Figures 5 (a, b, c), it is also possible to observe the change in the measurement of the average contact angles over 60 seconds (duration of the test), the images of the drops formed on each type of film, and the angles formed between the drop and the film at the initial instant recorded in the test.

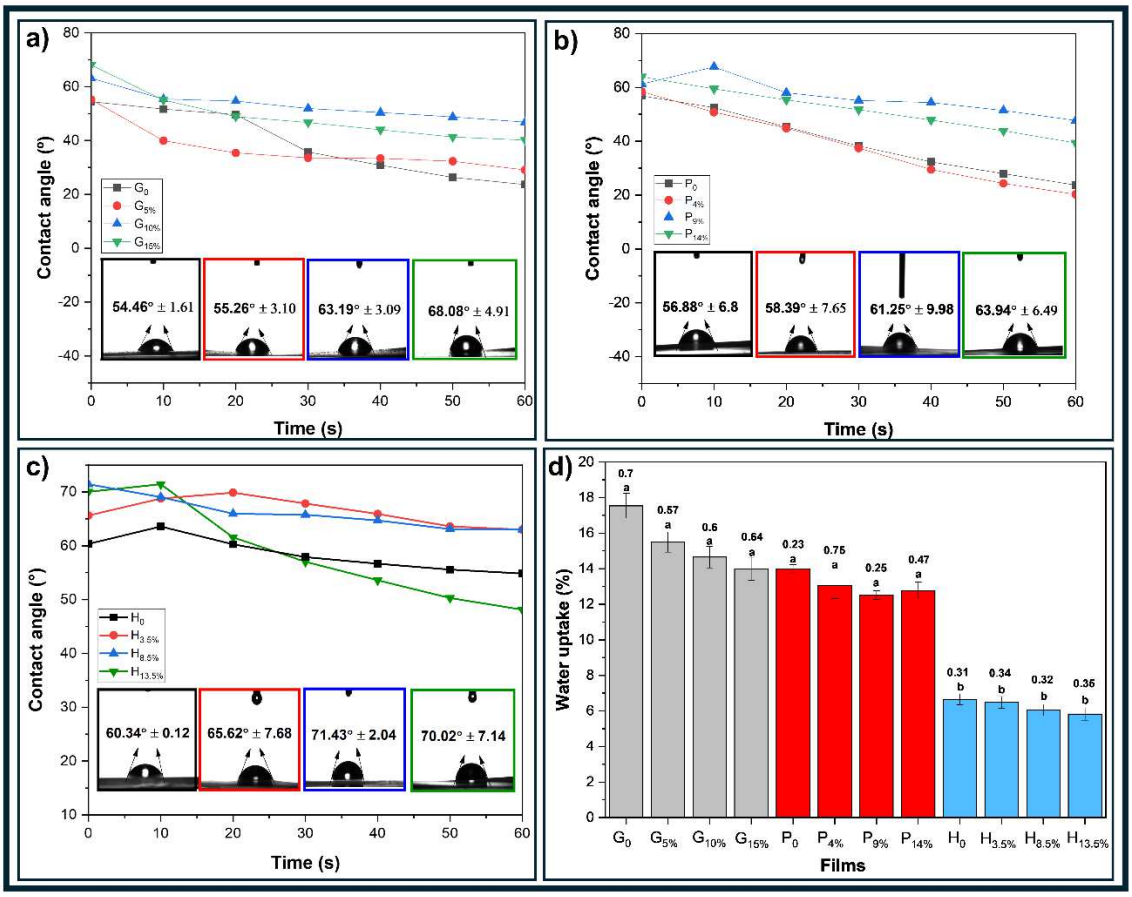

Figure 5: Contact angle of gelatin-based (a), pectin-based (b), and HPMC-based (d) biopolymeric nanocomposite films; and images of the droplets at 0 s. Moisture content of biopolymeric nanocomposite films (d). Values are expressed as mean ± SD (n = 9). Different superscripts within a column indicate significant differences between films ($p < 0.05$).

In liquid-solid interactions, a high angle (> 90°) indicates that water has a thermodynamic preference for interacting with its own molecules rather than with the material, in order to reduce surface free energy; however, the material surface is generally considered hydrophobic. On the other hand, a low angle (< 90°) allows liquids to slide easily across the surface, as adhesive forces overcome the fluid's cohesive forces; Therefore, the contact material has a hydrophilic nature [41, 42].

The average contact angle with water of the G_0 film surface was 54.46° (< 90°); therefore, the surface is hydrophilic. After the addition of 10% by mass of BCNCs, the average contact angle increased to 63.19°, and with 15% by mass of nanocrystals, the value rose to 68.08°. Thus, the reinforcement of BCNCs decreased the wettability and hydrophilicity of the gelatin-based films. However, the intrinsic average contact angle is less than 90°, which can be deduced from the wetting state [42].

For P_0, the average contact angle with water on the film surface was 56.88°, and in the biopolymeric nanocomposite films, the crystalline reinforcement allowed the values of the contact angles with water on the surface to increase moderately; however, the change was not significant. All contact angle values obtained indicate that the film surface is hydrophilic, due to the abundance of –OH groups present in the pectin structure [41].

In H_0, the average contact angle found was 60.34°. When adding 8.5% (71.43° ± 2.04), and 13.5% (70.02° ± 7.14) by mass of BCNCs to the HPMC matrix, a moderate increase in angles was observed. The higher value of the contact angle with water of the HPMC films occurred because the hydrogen bonding interactions between HPMC, and BCNCs increased the ability of HPMC to form hydrogen bonds with water. Yan et al. [29] reported that adding cellulose nanocrystals to the sodium alginate-based matrix decreased the hydrophilicity of the films, since the cellulose crystals were highly crystalline.

Among the gelatin, pectin, and HPMC matrices, HPMC-based biopolymeric nanocomposites showed better average contact angle values, which can be considered a potential material for application in films.

Water uptake

The ability of a film to be water uptake resistant is an essential property in packaging applications, especially for food items for storage; therefore, qualitative and/or quantitative determination in films is always of interest [41]. The water uptake results of the biopolymeric nanocomposites were investigated and are presented in Figure 5d.

Water molecules present in the films can affect the material's physical properties due to their strong plasticizing effect [33]. Gelatin, pectin, and HPMC are highly hydrophilic materials, which is one of their main drawbacks for packaging applications. Water can interact with the numerous hydrophilic groups—such as hydroxyl, carbonyl, and amino groups—present in these polymers; these groups render the polymers highly polar and, consequently, sensitive to water molecules, thereby altering the network organization [43]. As water absorption increases, water promotes greater mobility of the polymer chains and reduces the strength of interactions between adjacent chains, resulting in a structure that is more flexible and less cohesive [41, 44]. However, this characteristic is highly significant in facilitating the environmentally sound degradation of the materials [33].

Incorporating BCNCs into the polymer matrix generally results in improved performance, as the formation of a compact three-dimensional structure—mediated by hydrogen bonds between the polymer matrix and the nanocrystal molecules—limits water uptake (whether through chemical sorption, adsorption, or multilayer condensation), thereby reducing the likelihood of water molecules being retained within the structure [33, 45]. The G_0, $G_{5\%}$, $G_{10\%}$, and $G_{15\%}$ films exhibited moisture contents of 17.54%, 15.5%, 14.65%, and 14.0%, respectively. For the P_0 films, the value was 13.99%; with the addition of 4%, 9%, and 14% BCNCs by mass, moisture levels decreased to 13.06%, 12.51%, and 12.77%, respectively. It is observed that the addition of BCNCs reduced the moisture content of the films. This decrease in moisture was also observed in the study by Oyeoka et al. [33] involving the addition of NCs to gelatin/polyvinyl alcohol matrices. Incorporating NCs restricts polymer chain mobility, reduces the number of free hydroxyl groups in the matrix, and hinders water penetration into the molecular system [33].

HPMC films showed lower water uptake values compared to gelatin and pectin films. The moisture values obtained were 6.65%, 6.48%, 6.05%, and 5.83% for films H_0, $H_{3.5\%}$, $H_{8.5\%}$, and

$H_{13.5\%}$, respectively. Therefore, it is observed that the water uptake values decreased when nanocrystals were added. When adding 3.5% by mass of BCNCs, the moisture decreased (~2.56%), while adding 8.5% by mass of nanocrystals reduced the film moisture by 9.02%, and with 13.5% nanocrystals, the moisture decreased by 12.33%, compared to the control film. Dharmalingam and Anandalakshmi [46] showed in their studies that HPMC-based films have reasonable moisture levels. Pitpisutkul and Prachayawarakorn [47] reported that the moisture content of HPMC-based films is increased when associated with another hydrophilic natural polymer, as it exhibits excellent biocompatibility with a range of natural biopolymers.

Overall, the water absorption content of the biopolymeric nanocomposites decreased compared to the respective control films. This behavior, resulting from the addition of nanocrystals, inhibits film swelling by reducing the retention of water molecules [9, 33]. Thus, the incorporation of BCNCs aims not only to improve the physical properties of the films but also to enhance resistance to water absorption and ensure stability in high-humidity environments.

FT-IR spectra

Infrared spectroscopy is an important technique for determining chemical structural changes between and within molecules, which can be determined by the intensity and shift of absorption bands. Therefore, FTIR was applied to detect chemical interactions between the matrices and the reinforcing agent in the range of 400 to 4000 cm^{-1}. The infrared absorption spectra of the gelatin-based, pectin-based, and HPMC films, the respective biopolymeric nanocomposites of each matrix, and the BCNCs are shown in Figure 6.

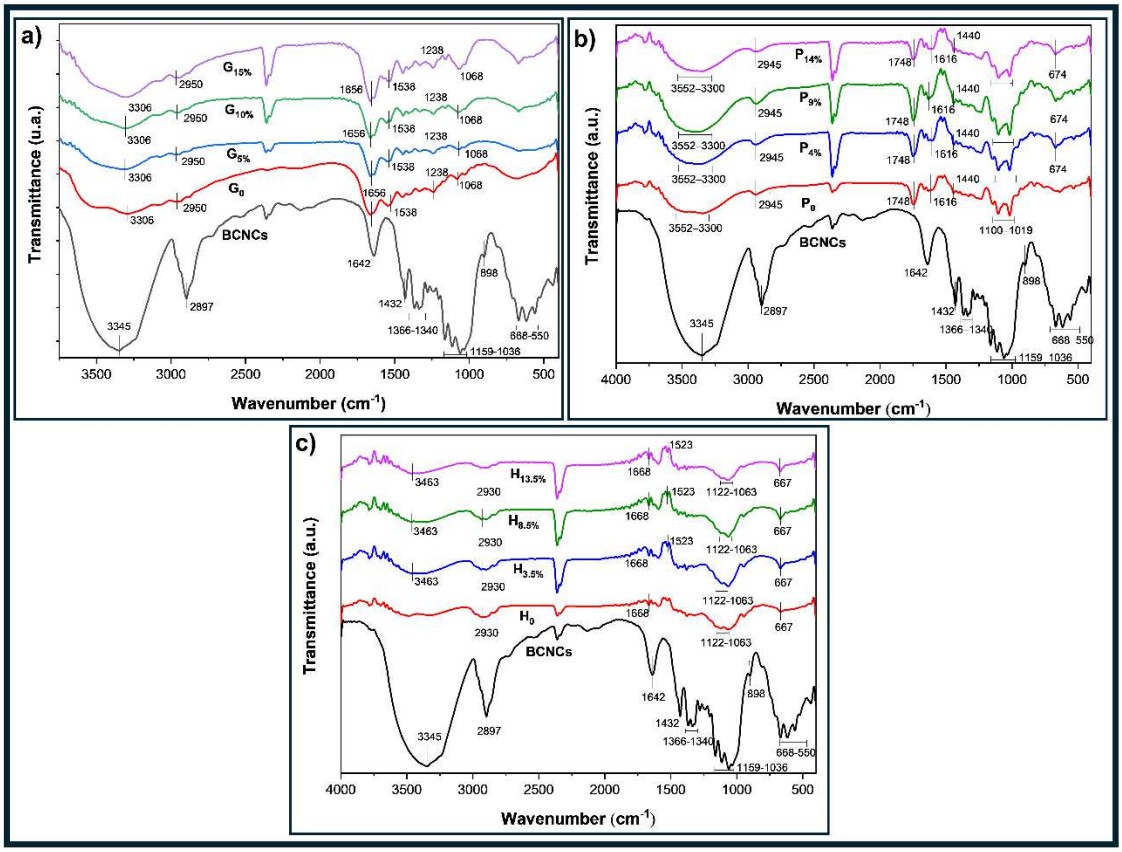

Figure 6: Absorption spectra in the infrared region of pure films, biopolymeric nanocomposites based on gelatin (a), pectin (b), and HPMC (c), and BCNCs.

Regarding the spectrum of BCNCs, a broad band can be observed around 3000−3700 cm^{-1} attributed to O-H stretching vibrations, present in BCNCs and water molecules, and bending vibrations of intra- and intermolecular hydrogen bonds [5, 33, 48]. Absorption related to C−H bond stretching can be observed at 2897 cm^{-1} [33], O−H bending vibrations of absorbed water at 1642 cm^{-1}, in-plane H−C−H and O−C−H bending vibrations at 1432 cm^{-1} [49], symmetrical angular deformation of C−H bonds between 1366, and 1340 cm^{-1} [50], C−O stretching vibrations between 1159 and 1036 cm−1, O−H bending in β−glycosidic bonds between anhydroglucose units at 898 cm^{-1}, and out-of-plane bending of C−OH between 668 and 550 cm^{-1} [49].

In the spectra of pure films and biopolymeric nanocomposites prepared with gelatin and BCNCs, an amide band was observed at 3306 cm^{-1} corresponding to the N–H and O–H elongation. A band at 2950 cm^{-1} is associated with the symmetric and asymmetric C−H modes [51]. The peak at 1656 cm^{-1} corresponds to the C=O stretching vibration of amide group I, while the peak at 1538 cm^{-1} is due to the coupling of the N−H bond and the elongation of the C−N bond of amide group II [31, 33]. The band at 1238 cm^{-1} belongs to amide III (N-H bending and C−N elongation) [30, 31]. C−O and N−H elongation, which correspond to the amide III bands, are exhibited by the peak designated at 1068 cm^{-1}. The addition of BCNCs hardly affects the peaks in the FTIR spectrum of the composite film.

In all spectra of pectin-based films, both pure pectin and biopolymeric nanocomposites, a broad band characteristic of hydroxyl group (−OH) stretching vibrations is present in the range of 3552−3300 cm^{-1} [52]. The peaks observed at 2946 cm^{-1} are related to C−H vibrations of galacturonic acid methyl esters in both pectin and biopolymeric nanocomposites [14]. The absorption band at 1748 cm^{-1} is attributed to −C=O stretching vibrations of ester ($-COOCH_3$) and carboxylate ion ($-COO^-$) [5, 53]. Furthermore, two additional vibrational bands related to carboxylic groups (COO^-) in their carboxylate form were observed in the spectra of the pure biopolymer films: asymmetric stretching at 1616 cm^{-1} and symmetric stretching at 1440 cm^{-1}. The spectral region below 1400 cm^{-1} encompasses the region containing a highly complex overlap of skeletal C−O and C−C vibrational bands of glycosidic bonds and pyranoid rings of polysaccharides [53].

Based on the spectra of HPMC-based biopolymeric nanocomposites, the O−H elongation vibration peak is at 3463 cm^{-1} [54], and the C−H stretching vibration peak in the $-CH_3$ and $-CH_2$ groups is at 2930 cm^{-1} [52]. For the methoxy group (CH_3O), the absorption band is exhibited at 1523 cm^{-1} [55]. The vibration related to the axial deformation of the C−O−C bond can be analyzed in the region between 1063 and 1122 cm^{-1}, and out-of-plane C−OH bending at 667 cm^{-1} [47, 49].

Obtaining information about the presence of BCNCs in the nanocomposite via FTIR analysis is particularly difficult, since both components are polysaccharides and therefore exhibit bands in the same wavenumber range [48].

Thermal properties

The thermal stability of the films, which reflects the material's ability to resist decomposition at high temperatures, was investigated by TG and DTG. Understanding thermal stability is relevant because the interactions between the raw materials of the films can also be determined from this characterization [14]. This property was evaluated in biopolymeric nanocomposites (one of each matrix).

The DTG thermograms (Figure 7b) were obtained by the first-order derivative of the TG curves (Figure 7a), which reflect the degradation rate.

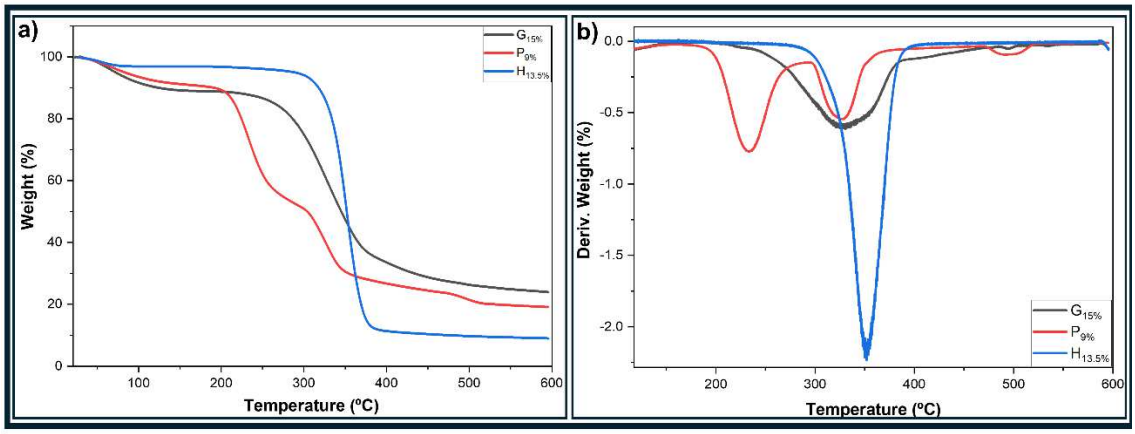

Figure 7: TG (a), and DTG (b) curves of gelatin, pectin, and HPMC-based films incorporating different levels of BCNCs.

All films exhibited mass loss in several stages during thermal decomposition from 20 to 600°C, which can be divided into events. The initial (T_i) and final (T_f) degradation temperatures and mass loss values associated with each thermal event for the biopolymeric nanocomposites are described in Tables 1 and 2.

Table 1 – Initial and final temperature values.

	Td_1 (°C)		Td_2 (°C)		Td_3 (°C)		Td_4 (°C)	
Films	T_i	T_f	T_i	T_f	T_i	T_f	T_i	T_f
$G_{15\%}$	31.1	138.3	244.3	392.3	488.6	500.1	-	-
$P_{9\%}$	36.5	146.5	210.3	255.2	316.3	343.4	490.1	500.5
$H_{13.5\%}$	35.2	84.1	295.9	389.5	-	-	-	-

T_i, T_f – Initial and final degradation temperature for each event. Td - Degradation temperature for each event.

Table 2 – Percentage of mass loss of the main degradation events of biopolymeric nanocomposites.

Films	**PM_1 (%)**	**PM_2 (%)**	**PM_3 (%)**	**PM_4 (%)**
$G_{15\%}$	11.1	54.0	10.8	-
$P_{9\%}$	8.7	32.7	27.6	11.8
$H_{13.5\%}$	3.1	87.8	-	-

P_M - Mass loss

It is possible to identify, from the curves represented in Figure 7b, 3, 4, and 2, degradation events for the $G_{15\%}$, $P_{9\%}$, and $H_{13.5\%}$ films, respectively.

The gradual mass loss in the first event, with initial temperatures around 31.1°C for $G_{15\%}$, 36.5°C for $P_{9\%}$, and 35.2°C for $H_{13.5\%}$, was caused by the volatilization of free water, i.e., water molecules not bound to the matrix [33, 51]. It is observed that the percentage of water molecules trapped in the HPMC films (average of 3.1%) is lower compared to the gelatin-based (11.1%) and pectin-based (8.7%) films, and this can be confirmed from Figure 5d, which represents the moisture content of the films. Therefore, the gelatin matrix retains a higher percentage of water molecules in its network, followed by pectin and HPMC.

The results presented in Figure 7a showed that gelatin and pectin-based biopolymeric nanocomposites are thermally stable in the region below 200°C, and for HPMC-based biopolymeric nanocomposites below 300°C, when a new stage of mass loss began. Therefore, in the second event, the percentage of mass loss for the $G_{15\%}$ film was 54.0%, $P_{9\%}$ 32.7%, and $H_{13.5\%}$ 87.8%. According to the results presented in Table 2 and Figure 7, HPMC, at this stage, showed the greatest mass loss, which is associated with the degradation temperature range of cellulosic materials (typical degradation profile of cellulose hydrolyzed with sulfuric acid) of the BCNCs and the matrix itself. The degradation of BCNCs generally occurs in two stages: degradation of highly sulfated and accessible amorphous regions around 150°C occurs first, followed by the breakdown of the non-sulfated bulk in the range of 250–500°C [56]. In addition to this event, the degradation of cellulose ethers is attributed to parallel dehydration and demethylation reactions of the HPMC chains [57]. For the gelatin-based biopolymeric nanocomposite, the second event, in the temperature range of 244.3–392.3 °C, is associated with the breakdown of the gelatin polymer chains [13, 51]. And for pectin-based biopolymeric nanocomposites, Sun, Wei and Xue [14] reported that in the temperature range of 120−280 °C, thermal degradation of the pectin chain backbone occurred, decomposition of the pectin backbone resulting from primary and secondary decarboxylation of pendant acid groups and carbon rings, and depolymerization reactions involving demethoxylation and hydrolytic cleavage.

In the third event, the mass loss of only 10.8% for the $G_{15\%}$ film was at an initial temperature of around 488.6°C, and for the $P_{9\%}$ film, 27.6% of the mass was degraded in T_i at around 316.3°C. For the gelatin-based film, this thermal event (temperature range 488.6–500.1 °C) is associated with carbon elimination [58]. And for the pectin film, this event is associated with the degradation (depolymerization, dehydration, and decomposition of glycosyl units) of the reinforcing agent (BCNCs) [33].

The fourth event for the $P_{9\%}$ film, which showed a mass loss of 11.8% at the initial temperature around 490.1°C, is also associated with carbon [58].

Studies have reported that biopolymer films reinforced with NCs have become more thermally stable. For example, Leite et al. [30] reinforced gelatin films with NCs, and based on the results found, they reported that gelatin films with a higher NCs content became more thermally stable, since the formation of hydrogen bonds between NCs and gelatin chains can influence the

protein denaturation process and the formation of triple helix crystalline structures, thus leading to an increase in the thermal stability of gelatin films.

Overall, the films exhibited high thermal decomposition temperatures, which allows them to remain stable in common food industry environments, and where the polymer mixing process requires high temperatures [58].

Biodegradability

Disintegration on the surface of natural soil

Biodegradation occurs as a result of the action of enzymes and/or chemical deterioration associated with living organisms, bacteria, or fungi [33, 59, 60]. This is generally followed by the assimilation of polymer fragments by microorganisms and their mineralization, during which they form carbon dioxide, water, methane, biomass, and mineral salts [61]. However, the International Organization for Standardization (ISO) and the American Standard for Testing and Materials (ASTM) designate it differently. According to ISO, any substance is considered biodegradable if its initial mass is reduced by 90% after six months under composting conditions at 58°C; however, ASTM describes a 60% reduction for homopolymers, and a 90% reduction for mixtures over a period of 180 days [59, 62, 63].

The biodegradability of packaging films is always desirable, as it is a natural process important for nutrient and energy recycling. To investigate the biodegradability of film residues based on gelatin, pectin, and HPMC, the samples were first placed on natural soil under controlled moisture and temperature conditions; changes were recorded to evaluate the disintegration potential of each film sample. Soil moisture was maintained at 35%—close to actual field conditions—as this better represents soil moisture in the various environments where most plastic waste accumulates. The samples were observed and photographed daily, but the images shown in Figure 8 represent those that exhibited the most significant differences in appearance.

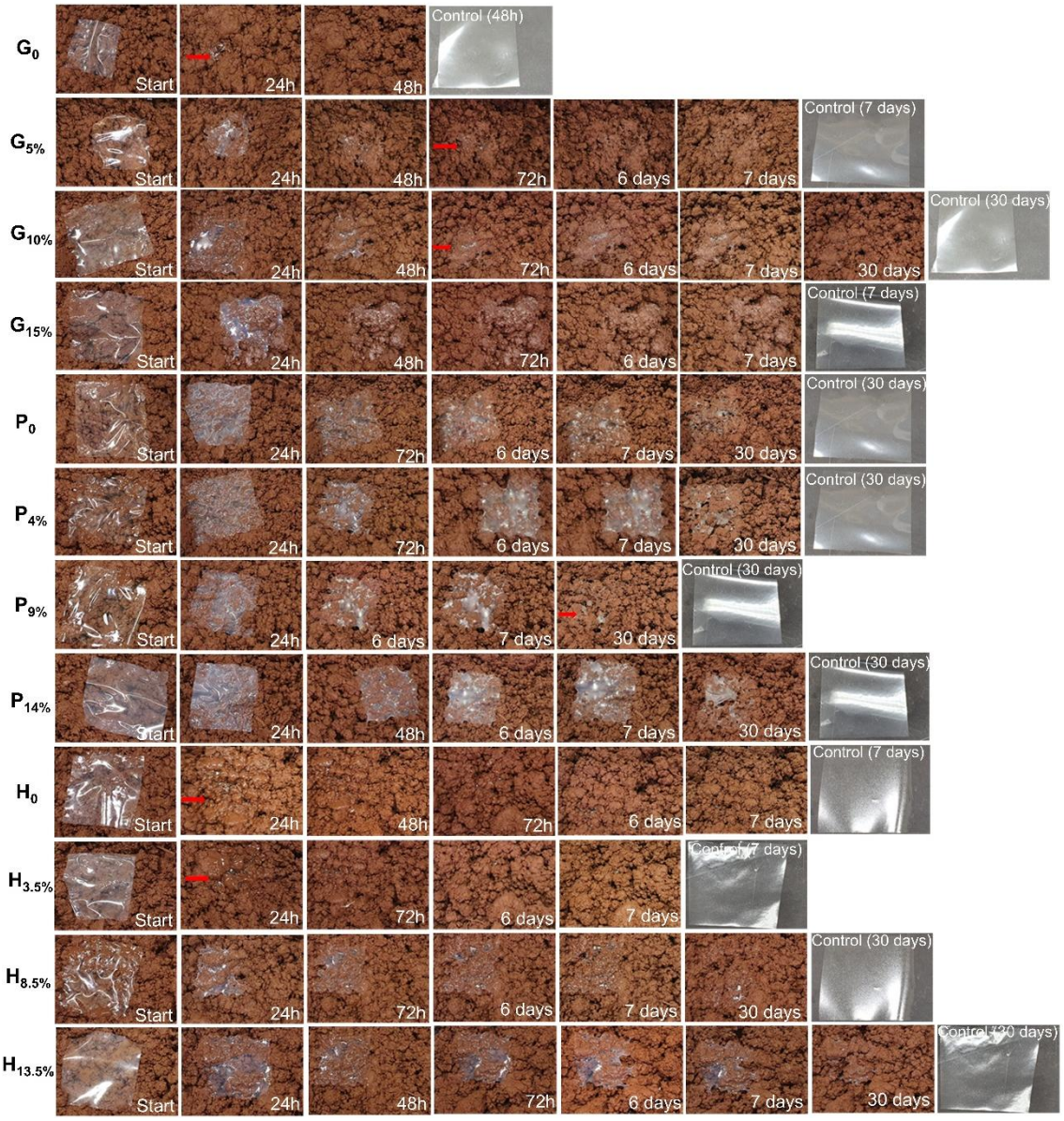

Figure 8: Images captured to observe the potential for disintegration of each film sample on the soil surface.

Soil surface disintegration tests were conducted over 30 days, and samples that did not fully disintegrate in this test were also subjected to composting disintegration analysis to evaluate the most satisfactory disintegration method. All films synthesized in this study were characterized for their biodegradation potential in natural soil.

The G_0 film disintegrated completely within 48 hours, whereas the gelatin-based biopolymeric nanocomposite film residues persisted for days before fully decomposing. The $G_{5\%}$ and $G_{15\%}$ films disintegrated within 7 days, while the $G_{10\%}$ film disintegrated within 30 days. All gelatin-based samples proved to be biodegradable. During the initial stage of the biodegradation process, the gelatin-based film residues gradually absorb water from the natural soil, and the matrix's hydrogen bonds are partially disrupted, resulting in a swollen state. The mixed microflora present in the natural soil gradually adheres to the surface of these films. Finally, the adhered mixed microflora slowly attacks the films until they are completely consumed [58].

The pectin-based films were more resistant to the disintegration process in natural soil. Figure 8 clearly shows that all samples, after 30 days, were not completely disintegrated. Sample $P_{14\%}$ was even more resistant to attack by microorganisms present in the soil compared to P_0, $P_{4\%}$, and $P_{9\%}$, due to the persistence of residual fragments.

HPMC-based films are more biodegradable in natural soil compared to pectin films and resemble gelatin films. The H_0 and $H_{3.5\%}$ samples completely disintegrated in 7 days, while the HPMC samples with 8.5% and 13.5% BCNCs by mass disintegrated almost completely in 30 days, leaving very few residue traces.

Several factors can hinder the biodegradation process of polymeric materials. These include crystallinity, polarity, interfacial polarization, and biotic and abiotic factors [60]. More organized (crystalline) polymer regions tend to impede enzymatic hydrolysis, as water molecules diffuse more easily through amorphous regions; consequently, catalytic proteins struggle to penetrate these crystalline areas [59]. Degrading microorganisms require a hydrophilic surface to adhere and catalyze the depolymerization reaction via hydrolytic enzymes [45]. Interfacial polarization can also occur due to the accumulation of generated charge carriers—such as ions, free electrons, and protons—at the interfaces between the various components of bioplastics; this instability in intermolecular interactions leads to bioplastic fragmentation [64]. Microbial populations (abiotic factors), as well as thermal, mechanical, and chemical degradation (abiotic factors), contribute to the various degradation processes [45].

Among the matrices studied, pectin exhibited the most organized molecular structure, and the incorporation of BCNCs further increased the crystallinity of the composite material's structure [3]. Consequently, the pectin-based biopolymeric nanocomposites demonstrated the highest resistance to disintegration.

Although the mass loss apparently due to degradation in 30 days is low for some biopolymeric nanocomposites, their high probability of complete biodegradation is an excellent attribute for packaging materials, especially for takeaway food packaging, which easily slips from disposal points and litters the streets [33].

Disintegration on the surface of the composting system

The biodegradation of biopolymers under composting conditions follows two simultaneous steps: hydrolytic degradation followed by biodegradation (microbial assimilation) [65]. According to Sánchez-Safont et al. [18], composting biodegradable plastic packaging appears to be one of the most promising solutions for waste management, given the difficulty of separating the organic fraction from urban waste.

Samples of biopolymeric nanocomposites $G_{10\%}$, P_0, $P_{4\%}$, $P_{9\%}$, $P_{14\%}$, $H_{8.5\%}$, and $H_{13.5\%}$ were also subjected to disintegration under composting conditions, as this procedure may be more efficient due to the alteration of biotic, and abiotic factors (temperature 55°C). Figure 9 illustrates the images recorded at 1, 3, 9, 14, 20, and 30 days. These samples were chosen for this analysis because the disintegration time occurred at or above the limit (30 days) of the study of biopolymeric nanocomposite disintegration on the surface of natural soil, under the following conditions: 35% moisture at 30°C.

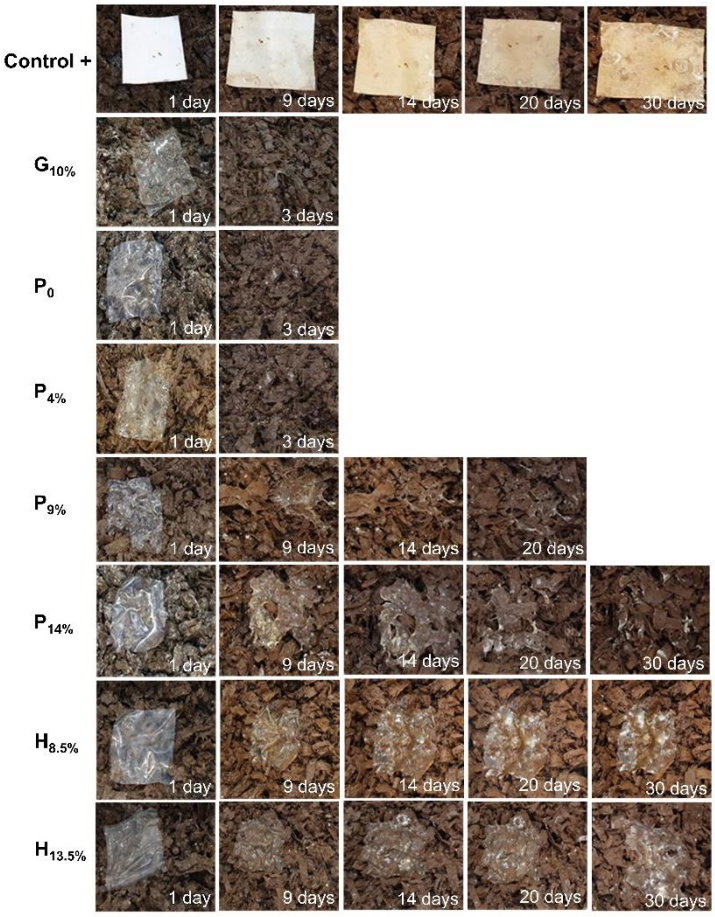

Figure 9: Disintegration by composting.

Samples $G_{10\%}$, P_0, and $P_{4\%}$ disintegrated in just 3 days of composting, while $P_{9\%}$ disintegrated in 20 days and $P_{14\%}$ disintegrated in 30 days with very little residue. For these samples, the composting disintegration method was more efficient compared to natural soil. Therefore, the accelerated disintegration time of the biopolymeric nanocomposites can be justified by the increase in the microbial population, and the temperature of the compost (which favors the disintegration process) (ABE et al., 2022).

This method was not advantageous for the $H_{8.5\%}$, and $H_{13.5\%}$ samples, as 30 days was not sufficient for complete disintegration. Therefore, disintegration in natural soil was more efficient, since few film fragments remained after 30 days. Hosseinnezhad et al. [60] noted that the complex structures of nanocomposites make disintegration challenging, and the chemical inertness of nanofillers limits depolymerization.

After 30 days of composting, the positive control (sulfite paper) showed no loss of mass, only a change in color (yellowing).

All biopolymeric nanocomposite formulations disintegrated in less time than indicated by ASTM 2003, and ISO 2012 [62, 63] standards when using the composting technique; therefore, all biopolymeric nanocomposites are biodegradable. The technique to be adopted is the one that is most convenient for the material. However, disintegration by composting is usually the most effective.

The development of films with low biodegradation/disintegration times shortens the life cycle of plastic materials in landfills, thus minimizing their environmental impacts [17].

Conclusion

The incorporation of bacterial cellulose nanocrystals (BCNCs)—derived from bacterial cellulose by-products of wound dressing production—enabled the creation of nanocomposite films based on gelatin, pectin, and HPMC, each exhibiting distinct responses to nanofiller concentrations near their respective percolation thresholds. The results demonstrated that the effect of BCNCs incorporation is not uniform across the matrices, being strongly influenced by the polymer's chemical nature, and structural organization.

Regarding barrier properties, BCNCs incorporation led to a significant reduction in water vapor permeability for pectin, and HPMC films, whereas the reduction observed in gelatin films was not statistically significant. This behavior suggests that the presence of a crystalline phase and the formation of tortuous paths can help restrict water vapor transport, though their efficiency depends on the interactions established between the BCNCs and the matrix. Concurrently, the incorporation of nanocrystals reduced the films' moisture content and moderately increased the water contact angle, although the surfaces remained predominantly hydrophilic. The water vapor permeability (WVP) results also highlighted the matrix's significant role, as the control films (gelatin, pectin, and HPMC) exhibited significant differences from one another.

Optical property analysis demonstrated that BCNCs incorporation can enhance the ultraviolet (UV) radiation barrier without substantially compromising transparency in the visible region. Even at relatively high nanocrystal concentrations, the films exhibited transmittances of approximately 97–100% at 600 nm, indicating that the filler's nanoscale dimensions allow the material's transparency to be maintained. The reduction in transmittance within specific UV regions is best attributed to radiation scattering caused by the presence and organization of the BCNCs structures.

FTIR analyses confirmed the presence of spectral characteristics associated with both the matrices and the BCNCs. Thermal results demonstrated that the films exhibited high decomposition temperatures, indicating sufficient stability for processing and application conditions compatible with packaging materials.

Disintegration behavior was a key aspect of the study, highlighting the strong influence of the matrix and BCNCs concentration. All gelatin-based films disintegrated in natural soil, whereas pectin films were more resistant—particularly the P14% formulation, which remained the most resistant after 30 days. HPMC films showed intermediate behavior: H_0 and $H_{3.5\%}$ disintegrated completely within seven days, while $H_{8.5\%}$, and $H_{13.5\%}$ showed only minor residues after 30 days. Under composting conditions, $G_{10\%}$, P_0, and $P_{4\%}$ disintegrated within three days; $P_{9\%}$ took 20 days, and $P_{14\%}$ took 30 days, whereas $H_{8.5\%}$, and $H_{13.5\%}$ did not fully disintegrate during the evaluated period.

Overall, the results demonstrate that forming a BCNCs network near the percolation threshold can modify water transport properties, surface interactions, optical response, and film

stability, but does not solely determine disintegration behavior. Matrix chemistry, structural organization, crystallinity, and BCNCs–polymer interfacial interactions play a fundamental role in defining the nanocomposite's final response. Thus, when selecting a material from the evaluated matrices, the desired set of properties must be considered: pectin showed greater resistance to disintegration, while BCNCs incorporation was particularly effective at reducing water vapor permeability in pectin and HPMC systems. Therefore, the results indicate that incorporating BCNCs allows for the tuning of biodegradable film properties, though the optimal nanofiller concentration must be determined based on the matrix and the specific requirements of the food packaging application.

Acknowledgements:

The authors would like to thank the USP - Universidade de Sao Paulo (University of São Paulo) and São Paulo State University (UNESP), São Paulo Research Foundation (FAPESP) (2025/09143-6; 2018/18697-1; 2013/03643-0; 2013/07296-2), and National Council for Scientific and Technological Development (CNPq) (CNPq) (MRM 408691/2023-9; 300986/2025-4; FAA 316174/2021-1; MCTIC Grant #406973/2022-9 through INCT/Polysaccharides – National Technology-Science Institute for Polysaccharides; and 307622/2023-1). This study was financed in part by the Coordenação de Aperfeiçoamento de Pessoal de Nível Superior – Brasil (CAPES) – “Finance Code 001.”

Declarations: The original contributions presented in this study are included in the article. Further inquiries can be directed to the corresponding author.

Conflict of interest: The authors declare no competing financial interests.

References

1. George J, Kumar R, Sajeevkumar VA, Ramana KV, Rajamanickam R, Abhishek V, Nadanasabapathy S, Siddaramaiah (2014) Hybrid HPMC nanocomposites containing bacterial cellulose nanocrystals and silver nanoparticles. Carbohydr Polym 105:285–292. https://doi.org/10.1016/j.carbpol.2014.01.057

2. Niskanen I, Zhang K, Karzarjeddi M, Liimatainen H, Shibata S, Hagen N, Heikkilä R, Yoda H, Otani Y (2022) Optical Properties of Cellulose Nanofibre Films at High Temperatures. Journal of Polymer Research 29:187. https://doi.org/10.1007/s10965-022-03019-0

3. da Costa FM, Melo PTS, Nishimoto PHK, Lorevice MV, Aouada FA, de Moura MR (2025) Percolation Threshold of Bacterial Nanocrystals in Biopolymeric Matrices to Build Up Strengthened Biobased Food Packaging. Foods 14:1123. https://doi.org/10.3390/foods14071123

4. Wang L, Auty MAE, Rau A, Kerry JF, Kerry JP (2009) Effect of pH and addition of corn oil on the properties of gelatin-based biopolymer films. J Food Eng 90:11–19. https://doi.org/10.1016/j.jfoodeng.2008.04.030

5. Akhila K, Ramakanth D, Rao LL, Gaikwad KK (2023) UV-blocking biodegradable film based on flaxseed mucilage/pectin impregnated with titanium dioxide and calcium chloride for food packaging applications. Int J Biol Macromol 239:124335. https://doi.org/10.1016/j.ijbiomac.2023.124335

6. Malik GK, Mitra J, Kaushal M (2023) Rheology of nano ZnO - Hydroxypropyl Methylcellulose (HPMC) based suspensions and structural properties of resulting films. J Food Eng 337:111187. https://doi.org/10.1016/j.jfoodeng.2022.111187

7. Wu J, Cui Q, Mi S, Yu W, Sang Y, Wang X (2026) Functional additives to strengthen composite packaging film containing cellulose nanocrystals: Property enhancement and applications in food preservation. Carbohydr Polym 371:124483. https://doi.org/10.1016/j.carbpol.2025.124483

8. Revin V V., Liyaskina E V., Parchaykina M V., Kuzmenko TP, Kurgaeva I V., Revin VD, Ullah MW (2022) Bacterial Cellulose-Based Polymer Nanocomposites: A Review. Polymers (Basel) 14:4670. https://doi.org/10.3390/polym14214670

9. Olusanya JO, Mohan TP, Kanny K (2023) Effect of nanoclay (NC) on mechanical and thermal properties of cellulose nanoparticles (CNPs) filled cornstarch bioplastic film. Journal of Polymer Research 30:262. https://doi.org/10.1007/s10965-023-03646-1

10. Azizi Samir MAS, Alloin F, Dufresne A (2005) Review of Recent Research into Cellulosic Whiskers, Their Properties and Their Application in Nanocomposite Field. Biomacromolecules 6:612–626. https://doi.org/10.1021/bm0493685

11. Ezati P, Khan A, Priyadarshi R, Bhattacharya T, Tammina SK, Rhim J-W (2023) Biopolymer-based UV protection functional films for food packaging. Food Hydrocoll 142:108771. https://doi.org/10.1016/j.foodhyd.2023.108771

12. Guo Z, Wu S, Lin J, Zheng H, Lei H, Yu Q, Jiang W (2023) Active film preparation using pectin and polyphenols of watermelon peel and its applications for super-chilled storage of chilled mutton. Food Chem 417:135838. https://doi.org/10.1016/j.foodchem.2023.135838

13. Li Y, Shan P, Yu F, Li H, Peng L (2023) Fabrication and characterization of waste fish scale-derived gelatin/sodium alginate/carvacrol loaded ZIF-8 nanoparticles composite films with sustained antibacterial activity for active food packaging. Int J Biol Macromol 230:123192. https://doi.org/10.1016/j.ijbiomac.2023.123192

14. Sun J, Wei Z, Xue C (2023) Preparation and characterization of multifunctional films based on pectin and carboxymethyl chitosan: Forming microchambers for high-moisture fruit preservation. Food Packag Shelf Life 37:101073. https://doi.org/10.1016/j.fpsl.2023.101073

15. Noronha VT, Camargos CHM, Jackson JC, Souza Filho AG, Paula AJ, Rezende CA, Faria AF (2021) Physical Membrane-Stress-Mediated Antimicrobial Properties of Cellulose Nanocrystals. ACS Sustain Chem Eng 9:3203–3212. https://doi.org/10.1021/acssuschemeng.0c08317

16. McHUGH TH, AVENA-BUSTILLOS R, KROCHTA JM (1993) Hydrophilic Edible Films: Modified Procedure for Water Vapor Permeability and Explanation of Thickness Effects. J Food Sci 58:899–903. https://doi.org/10.1111/j.1365-2621.1993.tb09387.x

17. Abe MM, Branciforti MC, Nallin Montagnolli R, Marin Morales MA, Jacobus AP, Brienzo M (2022) Production and assessment of the biodegradation and ecotoxicity of xylan- and starch-based bioplastics. Chemosphere 287:132290. https://doi.org/10.1016/j.chemosphere.2021.132290

18. Sánchez-Safont EL, González-Ausejo J, Gámez-Pérez J, Lagarón JM, Cabedo L (2016) Poly(3-Hydroxybutyrate-co-3-Hydroxyvalerate)/Purified Cellulose Fiber Composites by Melt Blending: Characterization and Degradation in Composting Conditions. J Renew Mater 4:123–132. https://doi.org/10.7569/JRM.2015.634127

19. Tavassoli M, Aslam R, Bahramian B, Abedi-Firoozjah R, Maqsood S (2026) Chlorogenic acid as a novel bioactive and functional ingredient in the fabrication of biodegradable food packaging films. Trends Food Sci Technol 172:105672. https://doi.org/10.1016/j.tifs.2026.105672

20. Wang X, Li S, Zeng M, Gong H, Zhang Z, Yuan X, Zhou M, Chen A, Liu Y, Wu H (2025) Preparation, characterization and application of antimicrobial pectin-konjac glucomannan composite films incorporating cellulose nanocrystals stabilized clove essential oil pickering emulsion. LWT 225:117855. https://doi.org/10.1016/j.lwt.2025.117855

21. Eichhorn SJ, Dufresne A, Aranguren M, Marcovich NE, Capadona JR, Rowan SJ, Weder C, Thielemans W, Roman M, Renneckar S, Gindl W, Veigel S, Keckes J, Yano H, Abe K, Nogi M, Nakagaito AN, Mangalam A, Simonsen J, Benight AS, Bismarck A, Berglund LA, Peijs T (2010)

Review: current international research into cellulose nanofibres and nanocomposites. J Mater Sci 45:1–33. https://doi.org/10.1007/s10853-009-3874-0

22. Melo PTS, Otoni CG, Barud HS, Aouada FA, de Moura MR (2020) Upcycling Microbial Cellulose Scraps into Nanowhiskers with Engineered Performance as Fillers in All-Cellulose Composites. ACS Appl Mater Interfaces 12:46661–46666. https://doi.org/10.1021/acsami.0c12392

23. Li S, Wang X, Wang J, Wang Z (2026) Dual-functional smart konjac glucomannan-based packaging incorporating gelatin-cellulose nanocrystal-stabilized emulsions and synergistic anthocyanin-curcumin dyes. Innovative Food Science & Emerging Technologies 109:104447. https://doi.org/10.1016/j.ifset.2026.104447

24. Leite LSF, Le Gars M, Azeredo HMC, Moreira FKV, Mattoso LHC, Bras J (2024) Insights into the effect of carboxylated cellulose nanocrystals on mechanical and barrier properties of gelatin films for flexible packaging applications. Int J Biol Macromol 280:135726. https://doi.org/10.1016/j.ijbiomac.2024.135726

25. Singh P, Baniasadi H, Gupta S, Ghosh R, Shaikh S, Seppälä J, Kumar A (2024) 3D-printed cellulose nanocrystals and gelatin scaffolds with bioactive cues for regenerative medicine: Advancing biomedical applications. Int J Biol Macromol 278:134402. https://doi.org/10.1016/j.ijbiomac.2024.134402

26. Wu H, Wang X, Li S, Zhang Q, Chen M, Yuan X, Zhou M, Zhang Z, Chen A (2024) Incorporation of cellulose nanocrystals to improve the physicochemical and bioactive properties of pectin-konjac glucomannan composite films containing clove essential oil. Int J Biol Macromol 260:129469. https://doi.org/10.1016/j.ijbiomac.2024.129469

27. Wu X, Prasad A (2025) Fundamental interactions between pectin and cellulose nanocrystals: a molecular dynamics simulation. Cellulose 32:5869–5887. https://doi.org/10.1007/s10570-025-06611-x

28. Jeong MY, Kim S, Kim HR, Jeon J, Won SS, Yang K-J, Park JS, Yang IG, Lee DG, Myung JH, Kim Y-G, Jin SG, Choi YS, Kim D-K, Kang MJ (2024) Dexamethasone nanocrystals-embedded hydroxypropyl methylcellulose hydrogel increases cochlear delivery and attenuates hearing loss following intratympanic injection. Carbohydr Polym 345:122546. https://doi.org/10.1016/j.carbpol.2024.122546

29. Yang J, Saqib MN, Liu F, Zhong F (2023) Bacterial cellulose nanocrystals with a great difference in aspect ratios: A comparison study of their reinforcing effects on properties of the sodium alginate film. Food Hydrocoll 141:108676. https://doi.org/10.1016/j.foodhyd.2023.108676

30. Leite LSF, Ferreira CM, Corrêa AC, Moreira FKV, Mattoso LHC (2020) Scaled-up production of gelatin-cellulose nanocrystal bionanocomposite films by continuous casting. Carbohydr Polym 238:116198. https://doi.org/10.1016/j.carbpol.2020.116198

31. Lin L, Mei C, Shi C, Li C, Abdel-Samie MA, Cui H (2023) Preparation and characterization of gelatin active packaging film loaded with eugenol nanoparticles and its application in chicken preservation. Food Biosci 53:102778. https://doi.org/10.1016/j.fbio.2023.102778

32. Yadav M, Behera K, Chang Y-H, Chiu F-C (2020) Cellulose Nanocrystal Reinforced Chitosan Based UV Barrier Composite Films for Sustainable Packaging. Polymers (Basel) 12:202. https://doi.org/10.3390/polym12010202

33. Oyeoka HC, Ewulonu CM, Nwuzor IC, Obele CM, Nwabanne JT (2021) Packaging and degradability properties of polyvinyl alcohol/gelatin nanocomposite films filled water hyacinth cellulose nanocrystals. Journal of Bioresources and Bioproducts 6:168–185. https://doi.org/10.1016/j.jobab.2021.02.009

34. Tien NNT, Nguyen HT, Le NL, Khoi TT, Richel A (2023) Biodegradable films from dragon fruit (Hylocereus polyrhizus) peel pectin and potato starches crosslinked with glutaraldehyde. Food Packag Shelf Life 37:101084. https://doi.org/10.1016/j.fpsl.2023.101084

35. Ren W, Qiang T, Chen L (2022) Recyclable and biodegradable pectin-based film with high mechanical strength. Food Hydrocoll 129:107643. https://doi.org/10.1016/j.foodhyd.2022.107643

36. Luo Q, Hossen MA, Zeng Y, Dai J, Li S, Qin W, Liu Y (2022) Gelatin-based composite films and their application in food packaging: A review. J Food Eng 313:110762. https://doi.org/10.1016/j.jfoodeng.2021.110762

37. Tyuftin AA, Kerry JP (2021) Gelatin films: Study review of barrier properties and implications for future studies employing biopolymer films. Food Packag Shelf Life 29:100688. https://doi.org/10.1016/j.fpsl.2021.100688

38. Yao L, Man T, Xiong X, Wang Y, Duan X, Xiong X (2023) HPMC films functionalized by zein/carboxymethyl tamarind gum stabilized Pickering emulsions: Influence of carboxymethylation degree. Int J Biol Macromol 238:124053. https://doi.org/10.1016/j.ijbiomac.2023.124053

39. Riahi Z, Hong SJ, Rhim J-W, Shin GH, Kim JT (2023) High-performance multifunctional gelatin-based films engineered with metal-organic frameworks for active food packaging applications. Food Hydrocoll 144:108984. https://doi.org/10.1016/j.foodhyd.2023.108984

40. Wu Y, Wu W, Farag MA, Shao P (2023) Functionalized cellulose nanocrystal embedded into citrus pectin coating improves its barrier, antioxidant properties and potential application in food. Food Chem 401:134079. https://doi.org/10.1016/j.foodchem.2022.134079

41. Wang P, Fei P, Zhou C, Hong P (2021) Stearic acid esterified pectin: Preparation, characterization, and application in edible hydrophobic pectin/chitosan composite films. Int J Biol Macromol 186:528–534. https://doi.org/10.1016/j.ijbiomac.2021.06.030

42. Hsieh P-C, Chien H-W (2023) Biomimetic surfaces: Insights on the role of surface topography and wetting properties in bacterial attachment and biofilm formation. Colloids Surf B Biointerfaces 228:113389. https://doi.org/10.1016/j.colsurfb.2023.113389

43. Jaramillo-Quiceno N, Rueda-Mira S, Marín JFS, Álvarez-López C (2023) Development of a novel silk sericin-based hydrogel film by mixture design. Journal of Polymer Research 30:120. https://doi.org/10.1007/s10965-023-03484-1

44. Bergo P, Moraes ICF, Sobral PJA (2013) Effects of plasticizer concentration and type on moisture content in gelatin films. Food Hydrocoll 32:412–415. https://doi.org/10.1016/j.foodhyd.2013.01.015

45. Abe MM, Branciforti MC, Brienzo M (2021) Biodegradation of Hemicellulose-Cellulose-Starch-Based Bioplastics and Microbial Polyesters. Recycling 6:22. https://doi.org/10.3390/recycling6010022

46. Dharmalingam K, Anandalakshmi R (2019) Fabrication, characterization and drug loading efficiency of citric acid crosslinked NaCMC-HPMC hydrogel films for wound healing drug delivery applications. Int J Biol Macromol 134:815–829. https://doi.org/10.1016/j.ijbiomac.2019.05.027

47. Pitpisutkul V, Prachayawarakorn J (2022) Hydroxypropyl methylcellulose/carboxymethyl starch/zinc oxide porous nanocomposite films for wound dressing application. Carbohydr Polym 298:120082. https://doi.org/10.1016/j.carbpol.2022.120082

48. de Moura MR, Lorevice M V., Mattoso LHC, Zucolotto V (2011) Highly Stable, Edible Cellulose Films Incorporating Chitosan Nanoparticles. J Food Sci 76:. https://doi.org/10.1111/j.1750-3841.2010.02013.x

49. Feng L, Zhang M, Hua Y, Zhu P, Tang Y (2023) Enhanced mechanical and thermal properties while maintaining transparency of epoxy resin film by introducing shear-oriented cellulose nanocrystals. Prog Org Coat 182:107683. https://doi.org/10.1016/j.porgcoat.2023.107683

50. Vasconcelos NF, Feitosa JPA, da Gama FMP, Morais JPS, Andrade FK, de Souza Filho M de SM, Rosa M de F (2017) Bacterial cellulose nanocrystals produced under different hydrolysis conditions: Properties and morphological features. Carbohydr Polym 155:425–431. https://doi.org/10.1016/j.carbpol.2016.08.090

51. Zhong Y, Zhang T, Zhang W, Wang G, Zhang Z, Zhao P, Liu X, Li H (2023) Antibacterial castor oil-based waterborne polyurethane/gelatin films for packaging of strawberries. Food Packag Shelf Life 36:101055. https://doi.org/10.1016/j.fpsl.2023.101055

52. Ren W, Luo C, Huang Y, Li S, Xu X, Gan J, Liu J, Zhao Z, Zou C, Zhao L, Liu B, Qiu F, Li X, Wang M, Guo B (2023) Hydroxypropylmethylcellulose: Functional material carrier for in-situ solid electrolyte engineering of advanced lithium metal batteries. Energy Storage Mater 59:102777. https://doi.org/10.1016/j.ensm.2023.102777

53. Moreira FK V., De Camargo LA, Marconcini JM, Mattoso LHC (2013) Nutraceutically Inspired Pectin–Mg(OH) 2 Nanocomposites for Bioactive Packaging Applications. J Agric Food Chem 61:7110–7119. https://doi.org/10.1021/jf402110g

54. Du Y, Hou X, Zhao J, Yuan X (2020) Effect of neutralization on physicochemical/mechanical properties of hydroxypropylmethylcellulose acetate succinate. Mater Chem Phys 249:122963. https://doi.org/10.1016/j.matchemphys.2020.122963

55. SandhyaRani N, Manjunatha MS, Sannappa J, Demappa T (2018) Studies of Hydrogen Bond between HPMC Doped CdCl2 Polymer using FTIR Technique. Mater Today Proc 5:22543–22546. https://doi.org/10.1016/j.matpr.2018.06.626

56. Dag D, Jung J, Zhao Y (2023) Development and characterization of cinnamon essential oil incorporated active, printable and heat sealable cellulose nanofiber reinforced hydroxypropyl methylcellulose films. Food Packag Shelf Life 39:101153. https://doi.org/10.1016/j.fpsl.2023.101153

57. Freitas PAV, de Oliveira T V, Silva RRA, Fialho e Moraes AR, Pires AC dos S, Soares RRA, Junior NS, Soares NFF (2020) Effect of pH on the intelligent film-forming solutions produced with red cabbage extract and hydroxypropylmethylcellulose. Food Packag Shelf Life 26:100604. https://doi.org/10.1016/j.fpsl.2020.100604

58. Chen L, Qiang T, Chen X, Ren W, Zhang HJ (2022) Gelatin from leather waste to tough biodegradable packaging film: One valuable recycling solution for waste gelatin from leather industry. Waste Management 145:10–19. https://doi.org/10.1016/j.wasman.2022.04.023

59. Amin U, Khan MKI, Maan AA, Nazir A, Riaz S, Khan MU, Sultan M, Munekata PES, Lorenzo JM (2022) Biodegradable active, intelligent, and smart packaging materials for food applications. Food Packag Shelf Life 33:100903. https://doi.org/10.1016/j.fpsl.2022.100903

60. Hosseinnezhad R, Khalaji M, Elumalai D, Vozniak I (2026) Sustainable recycling of polymer nanocomposites: Challenges and innovations. Advanced Industrial and Engineering Polymer Research 9:459–483. https://doi.org/10.1016/j.aiepr.2026.01.002

61. Ghasemlou M, Daver F, Murdoch BJ, Ball AS, Ivanova EP, Adhikari B (2022) Biodegradation of novel bioplastics made of starch, polyhydroxyurethanes and cellulose nanocrystals in soil environment. Science of The Total Environment 815:152684. https://doi.org/10.1016/j.scitotenv.2021.152684